

The effect of elevated intraocular oxygen on organelle degradation in the embryonic chicken lens

Steven Bassnett^{1,2,*} and Richard McNulty¹

¹Department of Ophthalmology and Visual Sciences and ²Department of Cell Biology and Physiology, Washington University School of Medicine, St Louis, MO 63110, USA

*Author for correspondence (e-mail: bassnett@vision.wustl.edu)

Accepted 14 August 2003

Summary

In the vertebrate lens, nuclei and other cytoplasmic organelles are degraded in fiber cells situated in the center of the tissue. This is believed to ensure the transparency of the tissue. The mechanism that triggers this process is unknown. We hypothesized that standing gradients of oxygen generated within the tissue may serve as a spatial cue for organelle degradation. To examine this possibility, we incubated fertilized chicken eggs under hyperoxic (50% O₂) or normoxic (21% O₂) conditions. Hyperoxic treatment was initiated on the seventh day of embryonic development (E7), five days before organelle degradation normally commences in the lens core. Hyperoxia was maintained until E17. Under normoxic conditions, the partial pressure of oxygen (P_{O_2}) within the vitreous compartment was low. Direct measurement of P_{O_2} using an optode oxygen sensor indicated values of 1.3 kPa and 0.4 kPa for the mid- and anterior vitreous, respectively. Similarly, treatment with pimonidazole, a bio-reductive hypoxia marker, led to the formation of immuno-positive

protein adducts within the lens, suggesting that the embryonic lens is chronically hypoxic *in situ*. Following hyperoxic treatment, vitreous P_{O_2} significantly increased, although pimonidazole staining in the lens was not markedly affected. Confocal microscopy of slices prepared from hyperoxic lenses revealed a significant increase in the size of the lens relative to age-matched normoxic controls. By E13, an organelle-free zone (OFZ) was present in the center of normoxic and hyperoxic lenses. However, in hyperoxic lenses, the OFZ was consistently smaller, and the distance from the lens surface to the border of the OFZ significantly larger, than in normoxic controls. These observations suggest that hyperoxia delays organelle breakdown and are consistent with a model in which hypoxia in the deep cortical layers of the normal lens serves as a trigger for the organelle loss process.

Key words: chicken, embryo, confocal microscopy, organelle, oxygen, optode.

Introduction

During lens fiber cell differentiation, all cytoplasmic organelles are degraded (Bassnett, 2002). In chicken lenses, this process begins in the central lens fibers on embryonic day 12 (E12). Thereafter, the resulting organelle-free zone (OFZ) of the lens expands at a rate of 80 $\mu\text{m day}^{-1}$ (Bassnett and Beebe, 1992), eventually encompassing most of the lens volume. Because the growth rate of the OFZ closely matches that of the embryonic lens, the border of the OFZ remains a fixed distance below the surface of the tissue. In embryonic chicken lenses, the OFZ border is located approximately 800 μm beneath the equatorial surface. In other species, the depth of organelle-containing cells varies considerably. For example, in the lens of the adult rhesus monkey, the organelle-containing layer is approximately 150 μm thick at the equator (Bassnett, 1997), while in the bovine lens this region may be more than 700 μm thick (R. McNulty and S. Bassnett, unpublished observation). In each case, however, the border is sharply defined. This implies that organelle breakdown is relatively rapid and synchronized in

a shell of fiber cells situated a specified distance below the lens surface.

It has been suggested that organelle loss may represent a form of attenuated apoptosis (Dahm, 1999). In support of this notion, biochemical studies have demonstrated the proteolysis of classical apoptotic substrates, such as PARP [poly(ADP-ribose)polymerase], during organelle loss (Ishizaki et al., 1998). Similarly, fiber cell nuclei become TUNEL-positive shortly before they disappear (Modak and Bollum, 1972), and an apoptotic-like DNA ladder is generated as the nuclei are broken down (Appleby and Modak, 1977). However, despite progress in elucidating the biochemical mechanism of organelle degradation, the signal that serves to trigger the process remains obscure.

Experiments with differentiating lentoid cultures suggested that organelle loss may be triggered through a death receptor pathway involving tumor necrosis factor α (TNF α). TNF α and two TNF α receptors (TNFR1 and TNFR2; Wride and Sanders, 1998) are expressed in the lens, but it is unclear how this

pathway might be activated specifically at the border of the OFZ, hundreds of cell layers beneath the lens surface. In the present study, we examine an alternative hypothesis.

The lens lacks a blood supply and has a limited and largely inaccessible (Shestopalov and Bassnett, 2000) extracellular space. Thus, metabolites entering or exiting the lens volume must do so across its surface. One consequence of this arrangement is that it leads, inevitably, to the generation of standing gradients of small, diffusible metabolites within the tissue. The magnitude of such gradients depends on the rate at which a metabolite is produced or consumed, the effective diffusion coefficient of the metabolite within the lens and the size of the lens. An example of this effect is the gradient of intracellular pH (pHi) observed within the lens. The lens obtains much of its ATP from anaerobic glycolysis (Winkler and Riley, 1991). Lactic acid generated by glycolysis diffuses from the lens only across its outer surface. Consequently, a standing gradient of lactic acid is established (Bassnett et al., 1987), resulting in values for core lens pHi that are significantly lower than those in the outer cortex (Bassnett and Duncan, 1986; Mathias et al., 1991).

Standing gradients may provide spatial cues that act to coordinate the differentiation process in fiber cells located within a growth shell. Of particular relevance in this regard may be the intralenticular distribution of molecular oxygen. Dissolved oxygen enters the lens from the aqueous and vitreous humors and is expected to diffuse rapidly through the tissue. Oxygen is consumed within the lens through oxidative phosphorylation within lens mitochondria and, perhaps, through non-mitochondrial mechanisms such as the oxidation of ascorbate. As a result, the partial pressure of oxygen (P_{O_2}) in the lens core is likely to be significantly lower than at the surface. In large lenses such as bovine or human lenses, where invasive measurements are feasible, we have observed such standing gradients of P_{O_2} (R. McNulty, R. Truscott and S. Bassnett, unpublished). Based on these observations, we hypothesize that as differentiating fiber cells become buried by more recently formed fibers, they will be subjected to increasingly severe hypoxia. Hypoxia has long been known to trigger apoptosis in a variety of cells (Banasiak et al., 2000) and, in the lens, we postulate that it may serve to trigger the related process of organelle degradation. To test this directly, in the present study we incubated chicken eggs under hyperoxic conditions (50% O_2). We reasoned that such treatment should increase intralenticular P_{O_2} and thereby inhibit the organelle loss process. The results indicate that hyperoxic treatment caused an increase in intraocular P_{O_2} and a partial inhibition of organelle loss. The data are consistent with the view that organelle loss may be triggered, at least in part, by a decline in intralenticular P_{O_2} .

Materials and methods

Animals

White Leghorn chicken (*Gallus gallus*) eggs (CBT Farms, Chestertown, MD, USA) were incubated in a humidified forced

draft incubator at 38°C until the seventh day of embryonic development (E7). At this point, some eggs were transferred to an airtight Plexiglas chamber (Bellco Glass Inc., Vineland, NJ, USA) located within the incubator. A mixture of humidified 50% O_2 :50% N_2 was passed continually through the chamber (flow rate, 50 ml min⁻¹). Eggs were removed from the chamber at E13, E15 or E17 and subjected to further analysis.

Microscopy

Embryos were decapitated and lenses were removed through an incision in the posterior globe. Lenses were fixed for two hours at room temperature in 4% paraformaldehyde/PBS (phosphate-buffered saline). Lenses were then embedded in 4% agar/PBS and sectioned in the sagittal plane at 100 µm intervals using a vibratome tissue processor (Model 100 plus; TPI, St Louis, MO, USA) as described (Bassnett, 1995). All slices were retained for further examination. Slices were stained for 1 h in 1 µg ml⁻¹ of acridine orange (Molecular Probes, Eugene, OR, USA) in PBS. Acridine orange binds to DNA and RNA. The latter is visible in acridine-stained tissue as diffuse cytoplasmic fluorescence. Because the levels of cytoplasmic RNA decline precipitously after the dissolution of the lens fiber nuclei, RNA staining provides a convenient method for delineating the borders of the organelle-free zone (OFZ). Following incubation in acridine orange, lens slices were washed for 1 h in PBS, coverslipped and viewed. Images were collected with an LSM 410 confocal microscope (Carl Zeiss Inc., Thornwood, NJ, USA) using the 488 nm laser line for excitation and a 515 nm long-pass filter for emission. Software provided with the microscope was used to measure the diameter of lens slices. The largest slice was deemed to be the midsagittal slice and was subjected to further analysis. The following parameters were measured from the confocal images: diameter and thickness of the lens, equatorial diameter and area of the OFZ, and distance from the border of the OFZ to the lens equator and poles (see Fig. 3C for clarification). Measurements were made on hyperoxic lenses and normoxic controls in a masked fashion.

Oxygen measurement

Vitreous P_{O_2} was measured using a fiber optic detection system (OxyLab, Oxford Optronix, Oxford, UK). The oxygen-sensing probe (optode) consisted of a 320 µm-wide optic fiber. An immobilized ruthenium-based fluorophore at the tip of the fiber served as the O_2 sensor. The sensor was illuminated with oscillating blue light. Fluorescence emitted by the O_2 sensor was transmitted by the fiber optic to the detector. Fluorescence lifetime was calculated automatically from the phase delay between the excitation and emission signals. The fluorescence lifetime of the fluorophore is inversely related to P_{O_2} , as described by the Stern–Volmer equation, and provides an accurate measure of P_{O_2} within the physiological range (Seddon et al., 2001). Optodes were obtained pre-calibrated by the manufacturer. To measure vitreous P_{O_2} , a hole was cut in the egg shell, and the head of the embryo was exposed. The fiber optic probe was inserted into the eye through the posterior sclera. A micromanipulator was used to position the optode tip

in the geometric center of the vitreous. Stable measurements were usually obtained within 20 s. After P_{O_2} was measured in the central vitreous, the optode tip was advanced to a position immediately behind the lens, where a second measurement was made.

Immunocytochemical detection of tissue hypoxia

Eggs were windowed to expose the head of the embryo. An injection of 3 μ l of a 10 mg ml⁻¹ solution of pimonidazole hydrochloride (hypoxyprobe-1; NPI, Inc., Belmont, MA, USA) was made into the left eye of the embryo. The egg was resealed for one hour and then the embryo was decapitated and the lens was removed and processed for histology. Immunocytochemistry was performed according to the instructions provided with the hypoxyprobe system. Briefly, following antigen retrieval with pronase, sections were incubated with a 1:50 dilution of hypoxyprobe Mab1, an antibody that specifically recognizes protein adducts formed by pimonidazole under hypoxic conditions. Antibody distribution was visualized with a horseradish peroxidase-conjugated secondary antibody, with diaminobenzidine (DAB) as the chromogenic substrate.

Results

An optode oxygen sensor was used to measure vitreous P_{O_2} in developing chicken embryos (Fig. 1). At early stages (<E9), due to the small size of the eye (and the relatively large diameter of the probe), a single measurement was made in the center of the vitreous. However, at >E9, eyes were large enough to allow separate P_{O_2} measurements in the mid-vitreous and the anterior vitreous. Oxygen levels in the developing eye of young embryos (\leq E8) were very low (0.7 kPa) but, by E9, had stabilized and did not change significantly thereafter. From E9 to E20, P_{O_2} in the mid-vitreous was 1.4 ± 0.1 kPa (mean \pm S.E.M., $N=11$). Anterior vitreous P_{O_2} was consistently lower than the mid-vitreous value. The mean anterior vitreous P_{O_2} from E9 to E20 was 0.4 ± 0.04 kPa.

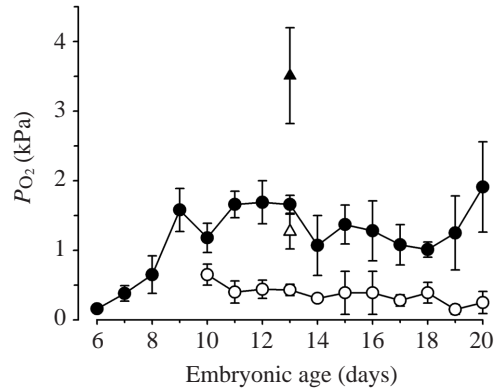


Fig. 1. Variation in intraocular oxygen partial pressure (P_{O_2}) during embryonic development and following treatment with 50% O_2 . An optode was used to measure P_{O_2} in the anterior vitreous (open symbols) and mid-vitreous (filled symbols) of normoxic chicken embryos (circles). Some embryos were incubated from E7 to E13 in an atmosphere of 50% O_2 :50% N_2 . Measurements made on those embryos (triangles), at E13, indicated that hyperoxia results in a significant increase in P_{O_2} in both the anterior and mid-vitreous.

We examined the effect on vitreous P_{O_2} of incubating eggs under hyperoxic (50% O_2) conditions. Eggs were incubated under normoxic conditions until E7 and then switched to hyperoxic conditions until E13. Measurements were made at E13 in the mid-vitreous and anterior vitreous of hyperoxic or normoxic control embryos (Fig. 1). Hyperoxia produced a significant elevation in P_{O_2} throughout the vitreous. In E13 hyperoxic embryos, the mid-vitreous P_{O_2} was 3.5 ± 0.7 kPa and the anterior vitreous P_{O_2} was 1.3 ± 0.2 kPa. These values were both significantly higher than those of normoxic controls ($P < 0.001$, $N=6$).

The optode oxygen sensor had a diameter of 320 μ m and, although this was sufficiently small to allow oxygen measurements in the vitreous humor, it was too large for intralenticular measurements. We therefore evaluated the use of a bioreductive hypoxia marker, pimonidazole, for visualizing the distribution of oxygen within the lens (Fig. 2). Preliminary experiments on E17

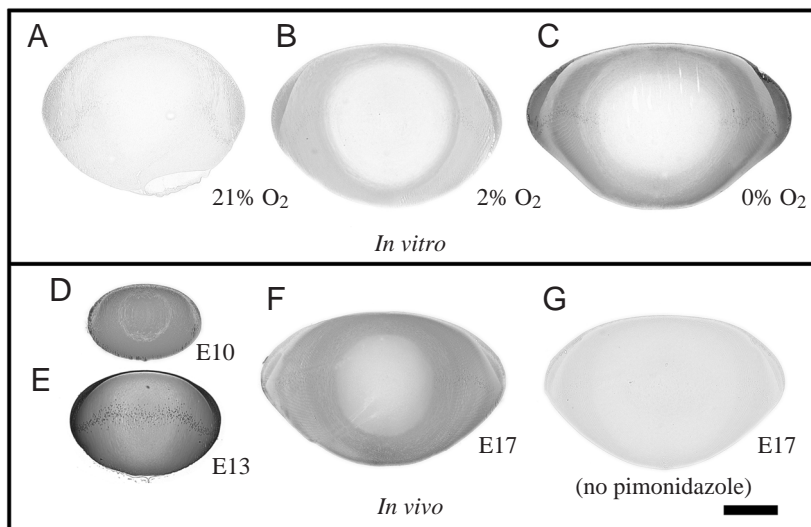


Fig. 2. Embryonic lens hypoxia visualized using the bioreductive marker pimonidazole. E17 lenses were incubated in pimonidazole *in vitro* (A–C) in solutions equilibrated with 21%, 2% or 0% O_2 . Formation of pimonidazole–protein adducts was visualized immunocytochemically (see text for details). In 21% O_2 (A), no adducts were detected. However, adducts were detected in the cortex of lenses incubated in 2% O_2 (B), and intense cortical staining was present in lenses incubated in 0% O_2 (C). *In vivo* treatment with pimonidazole (D–F) resulted in strong cortical immunostaining throughout development. When pimonidazole was omitted from the intraocular injection solution, no immunostaining was observed (G), confirming the specificity of the pimonidazole antibody. Scale bar, 250 μ m.

Table 1. Effect of hyperoxia on the formation of the organelle-free zone (OFZ) in the lens core

Embryonic age	%O ₂	Lens width (µm)	Lens thickness (µm)	Slice area (mm ²)	d1 and d2 (µm)	d3 (µm)	d4 (µm)	OFZ width (µm)	OFZ area (mm ²)	(OFZ area/slice area)×100
E13	21%	2251±77 (N=9)	1422±126 (N=9)	2.51±0.21 (N=9)	828±41 (N=18)	301±39 (N=9)	397±53 (N=9)	579±66 (N=9)	0.33±0.06 (N=9)	13.1±1.9% (N=9)
E13	50%	2337±36 (N=8)	1474±82 (N=8)	2.71±0.17 (N=8)	908±73 (N=16)	369±28 (N=8)	438±65 (N=8)	512±100 (N=8)	0.27±0.07 (N=8)	9.8±2.4% (N=8)
<i>t</i> -test		<i>P</i> =0.063	<i>P</i> =0.317	<i>P</i> =0.052	<i>P</i> =0.0006	<i>P</i> =0.0009	<i>P</i> =0.182	<i>P</i> =0.134	<i>P</i> =0.071	<i>P</i> =0.007
E15	21%	2577±62 (N=9)	1582±74 (N=9)	3.21±0.16 (N=8)	856±42 (N=18)	302±25 (N=9)	366±31 (N=9)	862±37 (N=9)	0.62±0.05 (N=9)	19.3±1.8% (N=9)
E15	50%	2610±77 (N=17)	1660±88 (N=17)	3.41±0.16 (N=17)	915±63 (N=34)	347±42 (N=17)	424±64 (N=17)	771±123 (N=17)	0.53±0.11 (N=17)	15.5±3.1% (N=17)
<i>t</i> -test		<i>P</i> =0.247	<i>P</i> =0.027	<i>P</i> =0.006	<i>P</i> =0.0002	<i>P</i> =0.002	<i>P</i> =0.005	<i>P</i> =0.01	<i>P</i> =0.008	<i>P</i> =0.0007
E17	21%	2775±132 (N=15)	1665±73 (N=15)	3.6±0.22 (N=15)	897±62 (N=30)	279±31 (N=15)	372±42 (N=15)	1019±96 (N=15)	0.81±0.09 (N=15)	22.5±1.6% (N=15)
E17	50%	2861±114 (N=11)	1862±86 (N=11)	4.12±0.27 (N=11)	961±58 (N=22)	352±27 (N=11)	434±34 (N=11)	947±47 (N=11)	0.79±0.06 (N=11)	19.2±1.0% (N=11)
<i>t</i> -test		<i>P</i> =0.184	<i>P</i> =0.002	<i>P</i> =0.007	<i>P</i> =0.0004	<i>P</i> =0.001	<i>P</i> =0.007	<i>P</i> =0.04	<i>P</i> =0.35	<i>P</i> =0.0001

Values are means ± S.E.M.

lenses *in vitro* demonstrated that pimonidazole–protein adducts were only formed in the lens under hypoxic conditions. Following incubation in solutions equilibrated with room air (20.9% O₂), no immunostaining was observed (Fig. 2A). However, incubation with solutions equilibrated with 2% O₂ resulted in diffuse staining of the lens cortex (Fig. 2B). In general, the most intense staining pattern was observed following incubation in solutions gassed with 100% nitrogen (0% O₂; Fig. 2C). In this case, the lens epithelium and cortex were strongly stained for pimonidazole–protein adducts. Parallel *in vivo* experiments indicated that the lens existed in a chronically hypoxic state throughout embryonic development. Thus, intraocular injection of pimonidazole at E10 (Fig. 2D), E13 (Fig. 2E) and E17 (Fig. 2F) resulted in adduct formation. In young embryos (<E13), adducts were present throughout the tissue. However, as with the *in vitro* experiments, at later stages (>E13) immunostaining was restricted to the lens cortex, and pimonidazole adducts were not detected in the lens core (Fig. 2F). Control experiments (Fig. 2G) confirmed that adduct formation was dependent on the presence of the pimonidazole. We examined whether incubation under hyperoxic (50% O₂) conditions abolished pimonidazole staining *in vivo*. Despite the fact that hyperoxia caused an approximate doubling of intraocular P_{O₂}, no change in pimonidazole–adduct staining within the lens was observed (data not shown).

We next determined the effect of hyperoxia on lens organelle loss, using acridine orange staining as a convenient method for visualizing the development of the OFZ (Fig. 3). In acridine orange-stained lens slices, cortical lens fiber cells were strongly fluorescent but, in contrast, the anucleated cells of the lens core were only weakly fluorescent (Fig. 3B). The acridine fluorescence reflected the relative concentrations of cytoplasmic RNA in various regions of the lens. At the ages examined here, the OFZ was approximately spherical, reflecting the organization of the fiber cells in the lens core. Along any given fiber cell the concentration of RNA was constant. Prolonged treatment with RNase A completely abolished the cytoplasmic staining (data not shown). Presumably, most RNAs were relatively short-lived, and because the anucleated fiber cells of the lens core were no longer transcriptionally active, the concentration of RNA within these cells rapidly decreased. The acridine orange fluorescence thus delineated the OFZ and allowed the various dimensions indicated in Fig. 3C to be measured (see Table 1).

To examine the effect of hyperoxia on organelle degradation, chicken eggs were incubated under normoxic (21% O₂) conditions until E7, at which point eggs were switched to 50% O₂ for a further 6, 8 or 10 days. In the embryonic chicken lens, organelle degradation commences in the central fiber cells on E12 (Bassnett and Beebe, 1992). Thus, embryos were exposed to hyperoxia for five days before the expected onset of organelle degradation and for various periods thereafter. Although extended exposure to hyperoxia is toxic in some settings, we did not observe any deleterious effects of 50% O₂ on the chicken embryos. There was no increased

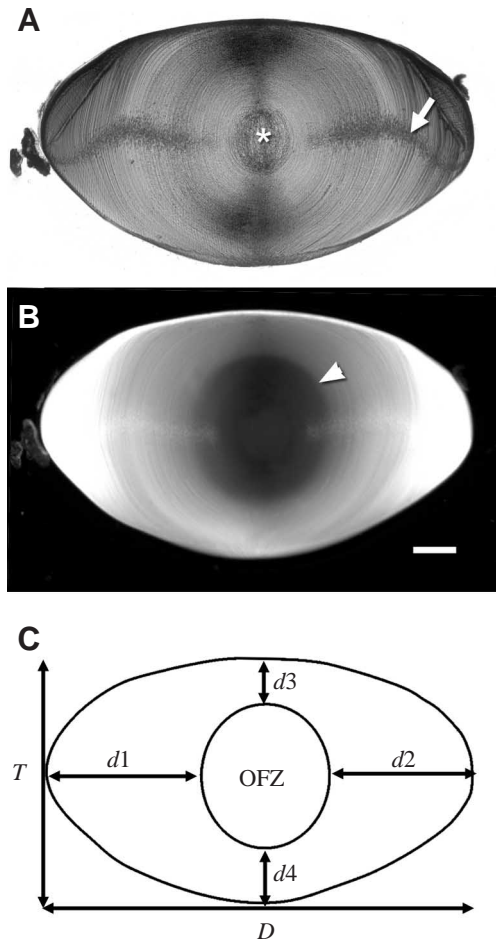


Fig. 3. Use of acridine orange to delineate the borders of the organelle-free zone (OFZ) in the developing chicken lens. (A) Midsagittal section of an E16 chicken lens. The lens is shown with its anterior surface facing up. The bulk of the lens is composed of elongated fiber cells arranged in concentric layers. Nuclei (arrow) are present in the peripheral cells but are absent from the oldest, innermost, fiber cells (asterisk). (B) Confocal image of the section shown in A, following incubation in $1 \mu\text{g ml}^{-1}$ acridine orange. Acridine fluorescence is strongest in the peripheral fiber cells. A clearly demarcated region with very low fluorescence is present in the center of the lens (arrowhead). This region corresponds to the OFZ. Scale bar, $250 \mu\text{m}$. (C) Tracing of the section shown in B, indicating the spatial parameters that were measured in this study to analyze the time course of organelle breakdown in the developing lens. d , distance; D , diameter; T , thickness.

tissue from normoxic controls. Hyperoxia caused a marked increase in the overall size of the lens (Fig. 4). At all ages examined, the mean diameter (D) of hyperoxic lenses was larger than that of normoxic controls, although the difference did not reach significance (Fig. 4A). The hyperoxic lenses were also consistently thicker (T) than the normoxic lenses, a difference that was more marked in the older embryos (Fig. 4B). Reflecting these differences in linear dimension, measurements of the area of midsagittal slices prepared from normoxic and hyperoxic lenses indicated that the latter were significantly larger at later embryonic ages (Fig. 4C).

A well-defined OFZ was present in the center of normoxic and hyperoxic lenses at the earliest time point examined (E13). Thus, hyperoxic treatment did not completely inhibit organelle breakdown. To examine whether hyperoxia subsequently delayed the organelle breakdown process, we measured the distance from the border of the OFZ to the equatorial or polar surfaces of the lens (Fig. 5). The distance from the lens equator to the OFZ border (mean of $d1$ and $d2$) did not vary greatly during development but was consistently and significantly greater in hyperoxic lenses compared with normoxic controls (Fig. 5A). In normoxic lenses, the ratio of this distance to the

mortality rate and the eyes of the hyperoxic embryos appeared to be completely normal. The effect of hyperoxia on the growth of the lens and the formation of the OFZ is shown in Figs 4–6 and Table 1.

Following incubation in elevated oxygen, lens slices were prepared, stained with acridine orange and compared with

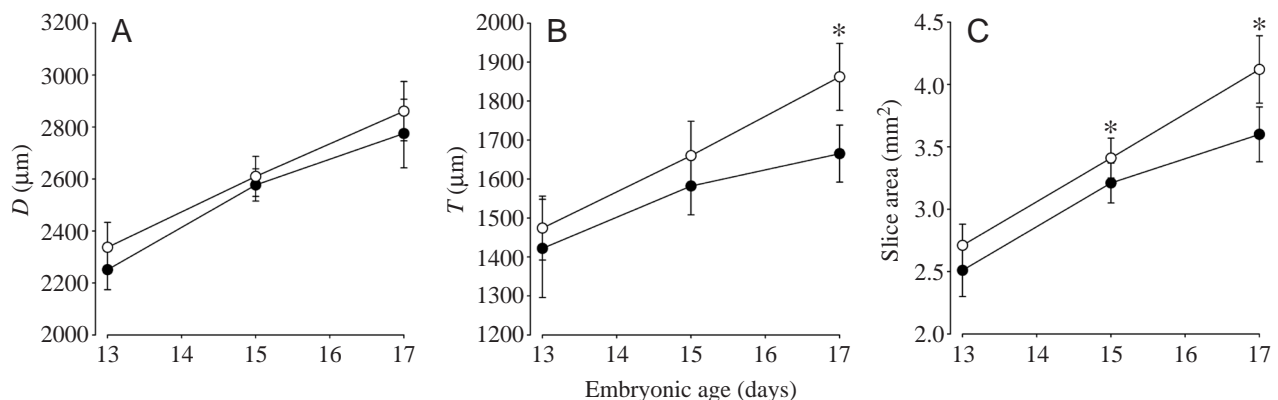


Fig. 4. Effect of hyperoxia on lens size. Beginning on E7, lenses were incubated in 50% O_2 :50% N_2 . Vibratome slices were prepared from hyperoxic or normoxic lenses and stained with acridine orange. (A) Lens diameter (D) is consistently larger in hyperoxic lenses (open circles) compared with normoxic controls (closed circles). (B) Lens axial thickness (T) is greater in hyperoxic lenses than in normoxic controls, and this difference reaches statistical significance by E17. (C) The area of mid-sagittal slices prepared from hyperoxic lenses is greater than normoxic controls. Asterisks denote significant ($P < 0.05$) difference between hyperoxic lenses and age-matched controls.

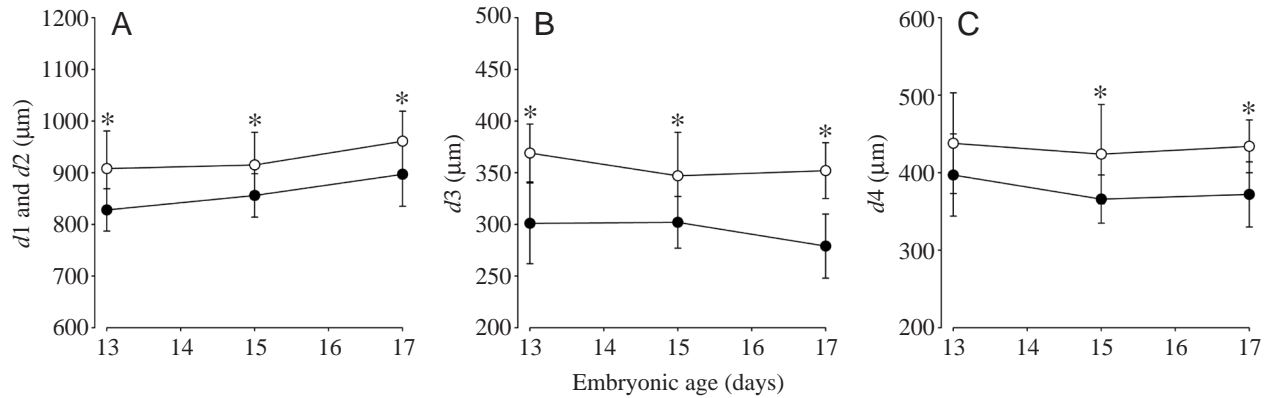


Fig. 5. Effect of hyperoxia on the distance from the lens surface to the border of the organelle-free zone (OFZ). (A) At all ages examined, the distance from the equatorial surface of the lens to the border of the OFZ ($d1$ and $d2$; see Fig. 3B) was significantly greater in hyperoxic lenses (open circles) compared with normoxic controls (closed circles). (B) Hyperoxia caused an increase in the distance from the anterior pole to the OFZ border ($d3$). (C) The distance from the posterior pole of the lens to the border of the OFZ ($d4$) was significantly greater in hyperoxic lenses.

total lens diameter fell from 0.37 at E13 to 0.32 at E17. In hyperoxic lenses, the ratio fell from 0.39 to 0.33 over the same period.

Similarly, the distance from the anterior or posterior pole to the border of the OFZ ($d3$ and $d4$, respectively) was relatively constant over the observation period but was always greater in the hyperoxic lenses (Fig. 5B,C). These data indicate that in hyperoxic lenses, organelle loss is triggered at a greater depth from the lens surface and thus at a later stage of differentiation than would ordinarily occur.

Finally, we examined the absolute and relative size of the OFZ formed in hyperoxic lenses (Fig. 6). Under hyperoxic conditions, the diameter of the OFZ was consistently smaller than under normoxic conditions (Fig. 6A), a difference that reached significance at later embryonic stages. The area of the OFZ in hyperoxic lenses was also consistently smaller than the normoxic controls (Fig. 6B), although the difference was only significant at E15. For each lens, the area of the OFZ was expressed as a percentage of the area of the lens slice. Under

both hyperoxic and normoxic conditions, the proportion of the slice area contained within the OFZ increased markedly during the observation period (Fig. 6C). However, in hyperoxic lenses, the OFZ accounted for a consistently smaller fraction of the total slice area than in normoxic controls.

Discussion

We employed a novel fluorescence lifetime-based assay to measure vitreous P_{O_2} . Our measurements revealed that P_{O_2} in the chicken vitreous was low (<2 kPa) throughout embryonic development. The P_{O_2} values recorded in the mid-vitreous were always significantly higher than those measured immediately behind the lens. Although, to the best of our knowledge, these are the first P_{O_2} measurements in an embryonic eye, similar standing P_{O_2} gradients have been noted in adult eyes in other species. For example, in rabbits, a vitreous P_{O_2} value of 0.3 kPa was measured behind the lens and 2.7 kPa adjacent to the retina (Ormerod et al., 1987). In

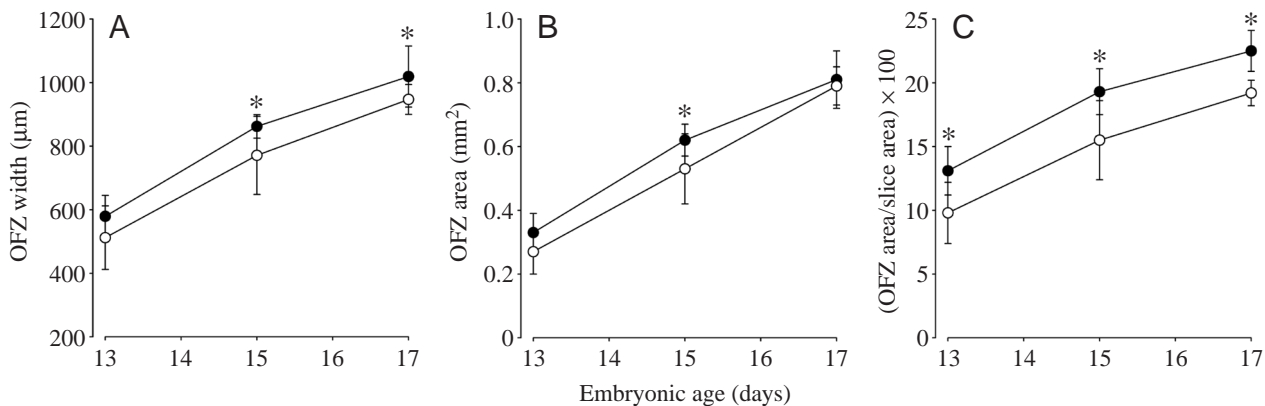


Fig. 6. Effect of hyperoxia on the dimensions of the organelle-free zone (OFZ). (A) The equatorial width of the OFZ is decreased by hyperoxia (open circles). (B) Hyperoxia caused a consistent decrease in the area of the OFZ compared with normoxic controls (filled circles). (C) For each lens slice, the fractional area occupied by the OFZ was calculated. In hyperoxic lenses, a significantly smaller fraction of the lens slice area was occupied by the OFZ.

humans, values of 2.1 kPa and 2.6 kPa have been reported for the central vitreous and posterior vitreous, respectively (Sakaue et al., 1989). These data probably reflect the fact that, in most vertebrates, the highly vascular retina represents a source of oxygen, and the lens a sink. Oxygen reaches the anterior lens from the iris vasculature. In adults, diffusion through the cornea is also a significant source of oxygen but this is probably less important in the embryonic eye. In adult humans, P_{O_2} values of 1.8 kPa have been recorded in front of the pupil (Helbig et al., 1993). Similar aqueous P_{O_2} values have been reported in rabbit and monkey eyes (Hoper et al., 1989). As with the vitreous humor, standing gradients of P_{O_2} have been measured in the aqueous humor of immobilized eyes (Helbig et al., 1993). However, these are likely to be dissipated by convective mixing in alert and active subjects (Maurice, 1998). Presumably, as with the vitreous humor, hyperoxic incubation results in an increase in aqueous humor P_{O_2} in the embryonic eye. However, the relatively small size of the anterior segment compared with the diameter of the optode precluded direct measurement of aqueous P_{O_2} in the present study.

Because of the small size of the embryonic lens (in young embryos, <1 mm in diameter), we used the hypoxia marker pimonidazole to visualize tissue hypoxia. Under hypoxic conditions, 2-nitroimidazole compounds form long-lived adducts in cells *in vivo* and *in vitro* (Hale et al., 2002; Raleigh et al., 1996; Varghese et al., 1976). Adducts form with thiol groups in proteins, peptides and amino acids and may be detected immunocytochemically. This approach has been used to visualize tissue hypoxia in the thymus (Hale et al., 2002), liver (Corpechot et al., 2002) and various types of tumors (Airley et al., 2003; Bennewith et al., 2002; Kaanders et al., 2002). As expected, pimonidazole adducts were produced in the lens *in vitro* under hypoxic (0% or 2% O_2) conditions. In young lenses, adducts were distributed throughout the lens; however, even in fully deoxygenated solutions, the cores of lenses from older embryos (>E13) were not stained by the adduct-specific antibody. The unstained region matched the OFZ in size and shape. It is likely that terminally differentiated fiber cells in the OFZ lacked the endogenous bioreductase activity necessary to properly metabolize the marker. It was not possible to quantify the pimonidazole staining as a function of P_{O_2} , in part because of uncertainties regarding the consumption of oxygen within the lens, and consequently the precise tissue P_{O_2} . However, pimonidazole-protein adducts are generally considered to form only at P_{O_2} values of <1.3 kPa (Varghese et al., 1976). Thus, the present results indicate that the embryonic lens was relatively hypoxic by E10 and remained so throughout development. Quantitative *in vivo* optode measurements of P_{O_2} in the vitreous humor immediately behind the lens supported this notion. The measured P_{O_2} in this region was <0.4 kPa. Despite an approximately threefold increase in P_{O_2} (to 1.3 kPa) following incubation in 50% O_2 , P_{O_2} in the fluids bathing the posterior surface of the lens remained below the 0.4 kPa threshold for pimonidazole adduct formation. This probably explains why

lenses from normoxic and hyperoxic embryos were stained similarly with the pimonidazole adduct-specific antibody.

Incubation in 50% O_2 was not associated with increased mortality or other obvious pathological change in the embryos. Careful measurements, however, revealed a slight but significant increase in the size of the lens relative to normoxic controls. This is consistent with earlier observations that established that the overall growth of chicken embryos was accelerated under hyperoxic conditions (van Golde et al., 1998) and that the mass of various organs systems, including the eye, was significantly greater than those in age-matched normoxic controls (McCutcheon et al., 1982; Stock et al., 1983). Furthermore, the degree of growth enhancement was shown to be proportional to the ambient oxygen concentration. Thus, treatment with 70% O_2 caused a greater increase than treatment with 40% or 60% O_2 (Stock et al., 1983). The fact that embryonic organ systems show a substantial growth response to elevated ambient O_2 suggests that increases in ambient P_{O_2} are associated in embryos with an increase in tissue P_{O_2} . Significantly, the vasoconstrictor response, which in adults serves to limit blood flow to organs under hyperoxic conditions, is lacking in embryos (van Golde et al., 1999). Although the lens was significantly larger in hyperoxic embryos than age-matched normoxic controls, we did not determine whether the increase reflected an increase in cell size, cell number or both.

The OFZ forms on E12 and expands thereafter. Because the expansion of the OFZ is closely matched by the growth of the tissue (Bassnett and Beebe, 1992), the depth of organelle-containing cells remains relatively constant during development (Fig. 5). Under normoxic conditions, the border of the OFZ is located 850 μm below the equatorial surface of the embryonic chicken lens (Fig. 5A). Under hyperoxic conditions, the border is situated approximately 100 μm further into the lens. This increase may be partly explained by the hyperoxia-induced increase in lens size but it is also associated with a real decrease in the size of the OFZ, suggesting that hyperoxia inhibits the organelle breakdown process in the deep cortical cell layers. The P_{O_2} in this region of the normoxic or hyperoxic lens was not quantitatively determined due to the very small size of the tissue. However, we postulate that, due to oxygen consumption in the outer layers, a standing gradient of P_{O_2} must be established within the lens and that organelle loss may be triggered when local P_{O_2} falls below a critical threshold value. Presumably, under hyperoxic conditions, this threshold value is encountered somewhat deeper into the lens.

Measurements made on other cellular conglomerates indicate that standing internal gradients of P_{O_2} (and other small metabolites) are an inevitable consequence of the avascular state. For example, in multicellular spheroids (a well-established *in vitro* model for solid tumors), growth of a spheroid invariably leads to progressive hypoxia in the core region (Dubessy et al., 2000). *In vitro*, multicellular spheroids show three phases of development (Dubessy et al., 2000). In the first phase, there is cellular proliferation throughout the spheroid and a concomitant increase in spheroid volume. In the

second phase, two cell layers are distinguished. The outer layer (also known as the viable rim) is proliferative and the inner layer is quiescent, due to diffusion-limited access to oxygen and nutrients and a decrease in pH. The final phase occurs when spheroids reach diameters of 200–500 μm . At this point, the accumulated metabolic deficits in the center of spheroids result in the formation of a necrotic core region (Carlsson et al., 1983). These phases are reminiscent of embryonic lens development. During lens development, cell proliferation is restricted to the peripheral layer of tissue. All cells are initially nucleated. However, when the lens polar diameter reaches approximately 1 mm, the cells in the lens core abruptly lose their nuclei in an apoptosis-like process. Thereafter, a thin rind of nucleated cells (resembling the viable rim of the spheroids) persists at the surface of the steadily growing tissue.

In summary, incubation of fertilized chicken eggs under hyperoxic conditions resulted in a marked increase in intraocular P_{O_2} and a significant increase in the depth of the organelle-containing layer of the lens. We hypothesize that an internal gradient of P_{O_2} , generated largely by mitochondrial oxygen consumption in the outer layers, may, in the inner layers, lead to mitochondrial dysfunction. Release of pro-apoptotic factors such as cytochrome *c* from oxygen-starved mitochondria may trigger an apoptosis-like cascade of events that results in breakdown of all cytoplasmic organelles. Because the effects of 50% O_2 treatment on the development of the OFZ were relatively modest, we endeavored to incubate embryos in either normobaric 100% O_2 or hyperbaric 100% O_2 , reasoning that such treatment might completely inhibit organelle degradation. Unfortunately, both treatments killed the developing embryos. Similarly, we reasoned that increased lens hypoxia might result in accelerated organelle degradation in the superficial layers of the lens. However, even brief exposure to hypoxic (10% O_2) conditions resulted in high mortality, as reported by others (Tazawa et al., 1992). The potential role of intralenticular P_{O_2} gradients in triggering organelle loss might, therefore, be better pursued in an organ culture setting. To our knowledge, however, no organ culture system has been described in which fiber cell differentiation and, in particular, organelle loss persist for an extended period *in vitro*.

The authors thank Dr Frank Giblin for his help with preliminary experiments and Peggy Winzenburger for her expert technical support. These studies were supported by NIH grants EY09852 and EY02687 (Core Grant for Vision Research) and an unrestricted grant to the Department of Ophthalmology and Visual Sciences from Research to Prevent Blindness. S.B. is an RPB William and Mary Greve Scholar.

References

- Airley, R. E., Loncaster, J., Raleigh, J. A., Harris, A. L., Davidson, S. E., Hunter, R. D., West, C. M. and Stratford, I. J. (2003). GLUT-1 and CAIX as intrinsic markers of hypoxia in carcinoma of the cervix: Relationship to pimonidazole binding. *Int. J. Cancer* **104**, 85-91.
- Appleby, D. W. and Modak, S. P. (1977). DNA degradation in terminally differentiating lens fiber cells from chick embryos. *Proc. Natl. Acad. Sci. USA* **74**, 5579-5583.
- Banasiak, K. J., Xia, Y. and Haddad, G. G. (2000). Mechanisms underlying hypoxia-induced neuronal apoptosis. *Prog. Neurobiol.* **62**, 215-249.
- Bassnett, S. (1995). The fate of the Golgi apparatus and the endoplasmic reticulum during lens fiber cell differentiation. *Invest. Ophthalmol. Vis. Sci.* **36**, 1793-1803.
- Bassnett, S. (1997). Fiber cell denucleation in the primate lens. *Invest. Ophthalmol. Vis. Sci.* **38**, 1678-1687.
- Bassnett, S. (2002). Lens organelle degradation. *Exp. Eye Res.* **74**, 1-6.
- Bassnett, S. and Beebe, D. C. (1992). Coincident loss of mitochondria and nuclei during lens fiber cell differentiation. *Dev. Dyn.* **194**, 85-93.
- Bassnett, S., Croghan, P. C. and Duncan, G. (1987). Diffusion of lactate and its role in determining intracellular pH in the lens of the eye. *Exp. Eye Res.* **44**, 143-147.
- Bassnett, S. and Duncan, G. (1986). Variation of pH with depth in the rat lens measured by double-barreled ion sensitive microelectrodes. In *The Lens: Transparency and Cataract* (ed. G. Duncan), pp. 77-85. Rijswijk, The Netherlands: EURAGE.
- Bennewith, K. L., Raleigh, J. A. and Durand, R. E. (2002). Orally administered pimonidazole to label hypoxic tumor cells. *Cancer Res.* **62**, 6827-6830.
- Carlsson, J., Nilsson, K., Westermark, B., Ponten, J., Sundstrom, C., Larsson, E., Bergh, J., Pahlman, S., Busch, C. and Collins, V. P. (1983). Formation and growth of multicellular spheroids of human origin. *Int. J. Cancer* **31**, 523-533.
- Corpechot, C., Barbu, V., Wendum, D., Chignard, N., Housset, C., Poupon, R. and Rosmorduc, O. (2002). Hepatocyte growth factor and c-Met inhibition by hepatic cell hypoxia: a potential mechanism for liver regeneration failure in experimental cirrhosis. *Am. J. Pathol.* **160**, 613-620.
- Dahm, R. (1999). Lens fibre cell differentiation – a link with apoptosis? *Ophthalmic Res.* **31**, 163-183.
- Dubessy, C., Merlin, J. M., Marchal, C. and Guillemin, F. (2000). Spheroids in radiobiology and photodynamic therapy. *Crit. Rev. Oncol. Hematol.* **36**, 179-192.
- Hale, L. P., Braun, R. D., Gwinn, W. M., Greer, P. K. and Dewhirst, M. W. (2002). Hypoxia in the thymus: role of oxygen tension in thymocyte survival. *Am. J. Physiol. Heart Circ. Physiol.* **282**, H1467-H1477.
- Helbig, H., Hinz, J. P., Kellner, U. and Foerster, M. H. (1993). Oxygen in the anterior chamber of the human eye. *Ger. J. Ophthalmol.* **2**, 161-164.
- Hoper, J., Funk, R., Zagorski, Z. and Rohen, J. W. (1989). Oxygen delivery to the anterior chamber of the eye – a novel function of the anterior iris surface. *Curr. Eye Res.* **8**, 649-659.
- Ishizaki, Y., Jacobson, M. D. and Raff, M. C. (1998). A role for caspases in lens fiber differentiation. *J. Cell Biol.* **140**, 153-158.
- Kaanders, J. H., Wijffels, K. I., Marres, H. A., Ljungkvist, A. S., Pop, L. A., van den Hoogen, F. J., de Wilde, P. C., Bussink, J., Raleigh, J. A. and van der Kogel, A. J. (2002). Pimonidazole binding and tumor vascularity predict for treatment outcome in head and neck cancer. *Cancer Res.* **62**, 7066-7074.
- Mathias, R. T., Riquelme, G. and Rae, J. L. (1991). Cell to cell communication and pH in the frog lens. *J. Gen. Physiol.* **98**, 1085-1103.
- Maurice, D. M. (1998). The Von Sallmann Lecture 1996: an ophthalmological explanation of REM sleep. *Exp. Eye Res.* **66**, 139-145.
- McCutcheon, I. E., Metcalfe, J., Metzberg, A. B. and Ettinger, T. (1982). Organ growth in hyperoxic and hypoxic chick embryos. *Respir. Physiol.* **50**, 153-163.
- Modak, S. P. and Bollum, F. J. (1972). Detection and measurement of single-strand breaks in nuclear DNA in fixed lens sections. *Exp. Cell Res.* **75**, 307-313.
- Ormerod, L. D., Edelstein, M. A., Schmidt, G. J., Juarez, R. S., Finegold, S. M. and Smith, R. E. (1987). The intraocular environment and experimental anaerobic bacterial endophthalmitis. *Arch. Ophthalmol.* **105**, 1571-1575.
- Raleigh, J. A., Dewhirst, M. W. and Thrall, D. E. (1996). Measuring tumor hypoxia. *Semin. Radiat. Oncol.* **6**, 37-45.
- Sakaue, H., Tsukahara, Y., Negi, A., Ogino, N. and Honda, Y. (1989). Measurement of vitreous oxygen tension in human eyes. *Jpn J. Ophthalmol.* **33**, 199-203.
- Seddon, B. M., Honess, D. J., Vojnovic, B., Tozer, G. M. and Workman, P. (2001). Measurement of tumor oxygenation: in vivo comparison of a luminescence fiber-optic sensor and a polarographic electrode in the p22 tumor. *Radiat. Res.* **155**, 837-846.
- Shestopalov, V. I. and Bassnett, S. (2000). Expression of autofluorescent

- proteins reveals a novel protein permeable pathway between cells in the lens core. *J. Cell Sci.* **113**, 1913-1921.
- Stock, M. K., Francisco, D. L. and Metcalfe, J.** (1983). Organ growth in chick embryos incubated in 40% or 70% oxygen. *Respir. Physiol.* **52**, 1-11.
- Tazawa, H., Hashimoto, Y., Nakazawa, S. and Whittow, G. C.** (1992). Metabolic responses of chicken embryos and hatchlings to altered O₂ environments. *Respir. Physiol.* **88**, 37-50.
- van Golde, J., Borm, P. J., Wolfs, M., Gerver, W. and Blanco, C. E.** (1998). The effect of hyperoxia on embryonic and organ mass in the developing chick embryo. *Respir. Physiol.* **113**, 75-82.
- van Golde, J. M., Mulder, T. A., Scheve, E., Prinzen, F. W. and Blanco, C. E.** (1999). Hyperoxia and local organ blood flow in the developing chick embryo. *J. Physiol.* **515**, 243-248.
- Varghese, A. J., Gulyas, S. and Mohindra, J. K.** (1976). Hypoxia-dependent reduction of 1-(2-nitro-1-imidazolyl)-3-methoxy-2-propanol by Chinese hamster ovary cells and KHT tumor cells in vitro and in vivo. *Cancer Res.* **36**, 3761-3765.
- Winkler, B. S. and Riley, M. V.** (1991). Relative contributions of epithelial cells and fibers to rabbit lens ATP content and glycolysis. *Invest. Ophthalmol. Vis. Sci.* **32**, 2593-2598.
- Wride, M. A. and Sanders, E. J.** (1998). Nuclear degeneration in the developing lens and its regulation by TNFalpha. *Exp. Eye Res.* **66**, 371-383.